Netherlands Journal of Geosciences — Geologie en Mijnbouw | 93 – 3 | 95-105 | 2014 doi: 10.1017/njg.2014.7

Measurements on the transport of suspended particulate matter in the Vlie Inlet

T. Gerkema[1,*], J.J. Nauw[1] & C.M. van der Hout[1]

1 NIOZ Royal Netherlands Institute for Sea Research, Texel

* Corresponding author. Email: gerk@nioz.nl

Manuscript received: 11 July 2013, accepted: 13 March 2014

Abstract

Results are presented from campaigns carried out in March and May 2012 across the main channel of the Vlie Inlet in the western Dutch Wadden Sea. On both occasions current velocities and concentrations of suspended particulate matter (SPM) were measured at six stations over one tidal cycle. Concentrations are found to be high only during late ebb and early flood, implying a brief but intense export and import of SPM, respectively. Transport of water and SPM occurs predominantly over the southwestern part of the channel. The tidal prism in the channel varies in the range of 5–7 $\times$ 10^8 m^3. Gross amounts of SPM transported during ebb and flood are 6–8 $\times$ 10^6 kg during the first campaign, but only half that amount during the second, possibly due to a different wind direction. The limitations encountered when calculating net effects over a tidal cycle are discussed, such as the fundamental indeterminacy in the duration of the tidal period itself.

Keywords: tidal inlet, sediment transport, tidal prism, optical backscatter

Introduction

The western Dutch Wadden Sea is connected to the North Sea by several tidal inlets (Fig. 1). Of these, the Marsdiep and Vlie are predominant in terms of tidal prism (mean tidal volumes). Louters & Gerritsen (1994) give as their values 1054 and 1078 million m^3, respectively; for the other inlets, the tidal prism is much smaller.

The Vlie is the oldest inlet. During the early Subatlanticum (~3000–1000 BP), it was the only pathway from the North Sea to the inner lake (Zagwijn, 1991), the later Zuiderzee and present IJsselmeer. Subsequently, human activities (such as peat excavation and compactification due to drainage) made the coastal areas more vulnerable for flooding. Around 1200 AD the Marsdiep was formed, opening up the western part of the Dutch Wadden Sea. This part is thus, by geological standards, very young. By this time, the rate of Holocene sea-level rise had already much declined and the rapid accumulation of sediment in the coastal zone, characteristic of the Atlanticum and Subboreal (~8000–3000 BP), was long over (Beets & van der Spek, 2000). This explains why this part of the Wadden Sea has a much lower coverage of intertidal flats.

Geological evidence suggests that barrier-island systems like the Wadden Sea are typically sedimentation areas (van Straaten, 1964). An important question is whether the Wadden Sea is presently a net importer of sediment from the North Sea. A recent analysis (for sand and silt together) suggests this to be the case: comparisons between bathymetric surveys from 1935 till 2005 show a net sedimentation (Elias et al., 2012). In part, this must be a response to the closure of the Zuiderzee in 1932; the main channels of Marsdiep and Vlie were cut short by the dyke and the remaining parts have since become shallower towards their landward edges.

An alternative and more direct way to look into the exchange of sediment between the North Sea and the Wadden Sea is by doing *in situ* measurements on the transports through the inlets. For suspended particulate matter (SPM) this requires simultaneous measurements of current velocities and concentration covering the whole vertical. Such measurements, however, are typically too short to warrant conclusions regarding the net balance of the Wadden Sea; they merely provide a snapshot of what actually is an episodic process in the long run. Van Straaten (1975) outlined the role of two opposing effects that play on different time scales: on the one hand, weak net imports

https://doi.org/10.1017/njg.2014.7 Published online by Cambridge University Press

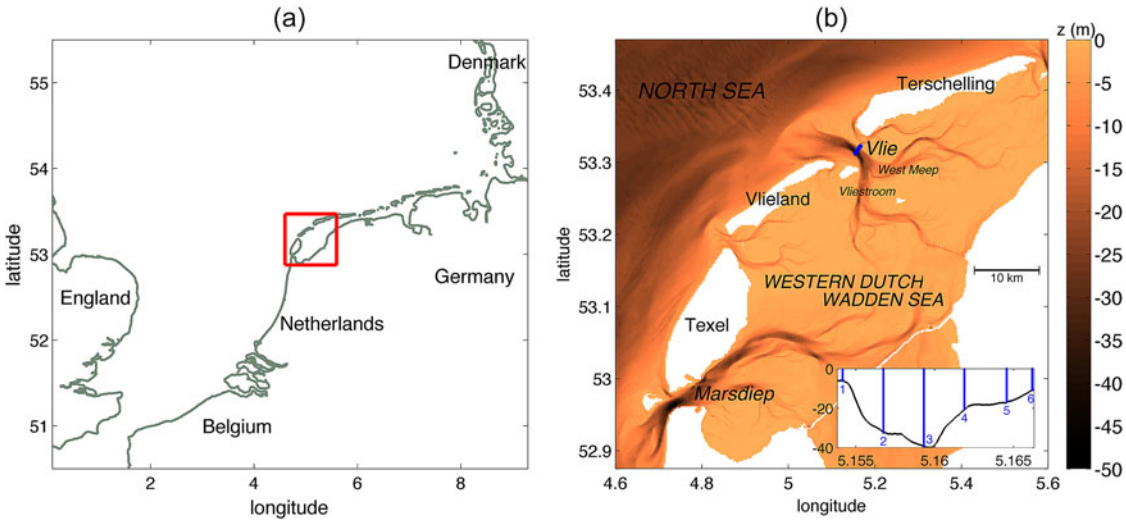

Fig. 1. (a) The location of the Western Dutch Wadden Sea is indicated by the red rectangle. Its bathymetry is shown in (b), with depth in metres. The transect of the six stations in the Vlie is indicated as a blue line. All points higher than 1 m above NAP are considered to be 'land' in this figure and are rendered white. The inset shows the profile of the main channel of the Vlie (depth vs longitude, based on our ADCP measurements) along with the six stations.

by tidal currents during periods of predominantly calm conditions and, on the other hand, large but brief exports during heavy storms, when silt is washed off the intertidal flats. It is the net effect of these two that ultimately determines the long-term evolution. To capture this net effect, *in situ* measurements would need to be sustained over periods of years. At present, this is done only in the Texel Inlet, Marsdiep (Nauw et al., 2014).

This leaves us with a gap of knowledge regarding the other potentially important inlet, the Vlie. A current research project (ZKO *PACE*) aims to examine the transport of SPM in the Wadden Sea using numerical models (GETM/GOTM and Delft3D). In support of this effort, we carried out two 13-hour measurements across the main channel of the Vlie Inlet, on 22 March and 15 May 2012, using the NIOZ R/V Navicula. This involved current velocities measured with an acoustic doppler current profiler (ADCP), vertical profiles of optical backscatter (OBS), and water samples and filtering to determine SPM concentrations. The results are reported in this paper.

The main objective of these measurements lies in estimating the gross import and export during a tidal cycle, rather than in their difference, the net effect. From the preceding discussion it will already be clear that net amounts of transport of SPM over one tidal cycle, even if we were able to reliably infer them from the measurements, would not be indicative of the long-term evolution of the Vlie basin. Moreover, the fundamental question arises whether such net quantities can be properly determined in the first place; upon closer inspection, 'the' tidal period (the duration over which the net effect is to be calculated) is an ambiguous concept, as we will discuss below.

The purpose of these 13-hour measurements is thus twofold: first, to get a synoptic view of the temporal and spatial variability of the transport of SPM within a tidal cycle and, second, to obtain estimates of the amounts of SPM involved in the gross import and export during that cycle. This provides crucial data against which future models can be tested.

Study area

The Vlie inlet, measured from island to island, has a width of 7.6 km. This poses a hurdle for doing *in situ* measurements: if the entire stretch were covered, the sampling within the tidal cycle would be insufficient. For this reason we restricted our measurements to the main channel, at a location where it is at its narrowest. The six stations are shown in Fig. 1 and their coordinates are given in Table 1; they cover a distance of 1.4 km. Over this stretch, every station can be sampled some 12 times during the 13-hour measurements. The obvious limitation of this approach is that we will miss an unknown but certainly significant part of the transports through the inlet, namely those over adjacent flats and through some smaller channels that are also part of the Vlie Inlet.

The 13-hour measurements were carried out along the same transect on 22 March and 15 May 2012. On 22 March, 12 crossings were made from stations 1 to 6 (and return crossings without casts). On 15 May, 10 crossings were made. Near the end of

Table 1. Position and waterdepth of the stations.

Station	Longitude	Latitude	Depth (m) 22 March	Depth (m) 15 May
1	5° 09.249′	53° 18.725′	6.4 ± 0.2	7.1 ± 0.8
2	5° 09.404′	53° 18.858′	32.6 ± 0.5	32.1 ± 0.5
3	5° 09.558′	53° 18.989′	39.6 ± 0.5	39.9 ± 0.8
4	5° 09.712′	53° 19.121′	20.8 ± 0.9	20.4 ± 0.9
5	5° 09.873′	53° 19.256′	17.0 ± 0.2	16.9 ± 0.2
6	5° 09.970′	53° 19.341′	11.0 ± 0.3	10.8 ± 0.6

The waterdepth (with respect to NAP) is based on ADCP data together with data from the tidal gauge at Vlieland Haven to correct for sea-level variations (tides and wind surges).
The errors indicate standard deviations.

https://doi.org/10.1017/njg.2014.7 Published online by Cambridge University Press

Table 2. Tidal characteristics.

	22 March	15 May
High water (predicted)	7:56 (+72)	15:25 (+80)
High water (measured)	7:50 (+56)	15:40 (+101)
Slack (flood to ebb)	9:00	-
Low water (predicted)	14:00 (-126)	9:06 (-100)
Low water (measured)	14:20 (-141)	9:20 (-82)
Slack (ebb to flood)	15:04	10:20

Predictions and measured high/low waters are for Vlieland Haven (data from RWS). The water level is mentioned in brackets, in centimetres with respect to NAP. Predicted values are based purely on tidal components and do not include wind surges. Measured sea levels are given only once every 10 min and so have that margin of uncertainty for the times of measured high and low waters. Times of slack are based on the measurements presented here, calculated for the bulk water transport. The turn from flood to ebb on 15 May fell after the campaign was halted. All times are in UTC.

the second campaign, a combination of strong winds and flood currents made it impossible to stay close to stations during the casts; at that point the campaign had to be halted and the last intended crossing was dropped.

The conditions were different with regard to both wind and tides. On 22 March, the wind was more or less perpendicular to the channel, ENE 4–5 Bft. It was two days before spring tides (new moon on 22 March, 14:37 UTC). On 15 May, the wind was stronger and directed straight into the inlet: NW 5 Bft, increasing to NNW 7 Bft in the afternoon. Neap tides fell on this day (last quarter on 12 May, 21:47 UTC).

The tidal characteristics are summarised in Table 2. We see that slacks come shortly after high or low waters (within about an hour or less), so already at this location the tides are closer to a standing than to a propagating wave. In line with the prevailing wind directions, water levels were lower than predicted on 22 March and higher than predicted on 15 May (see values in brackets, Table 2).

Instruments and data handling

From OBS to SPM

CTD/OBS vertical profiles (with Seabird/Seapoint sensors; CTD, conductivity temperature depth) were taken at all stations during each crossing from stations 1 to 6 (but not during return crossings). Water samples (using a Niskin bottle) were taken at stations 1, 3 and 5, both at the surface and at the bottom. Subsamples were filtered (oven dried and pre-weighed filters), and subsequently dried and weighed to obtain the concentration of SPM. The Niskin bottle, however, was on a different winch than the CTD/OBS frame and therefore at a different position in the water, so these SPM values cannot be directly used to translate the OBS profiles into SPM profiles. To connect them, we also measured the OBS value for each water sample, using another OBS sensor in the laboratory on board the ship. A calibration between the two OBS sensors then allowed us, finally, to translate OBS profiles from the CTD/OBS frame into OBS values of the sensor in the laboratory, and hence into SPM concentrations. The procedure is described in more detail by Merckelbach & Ridderinkhof (2006).

The main uncertainty in this procedure lies in the relation between SPM concentrations and OBS values (taken from the same sample in the laboratory), as illustrated in Fig. 2. The data show considerable scatter and are heteroskedastic, i.e. the dispersal of points is uneven: the spreading becomes larger for larger values. In such cases, with errors not being random, the Theil–Sen method is more appropriate than the commonly used least-squares method (e.g. Sprent 1993), so we adopted the former. The Theil–Sen method is also less sensitive to outliers.

For 15 May, the steepness of the linear fit is only 70% of that for 22 March. This is possibly related to the fact that current velocities were higher on 22 March (e.g. blue lines in Fig. 7),

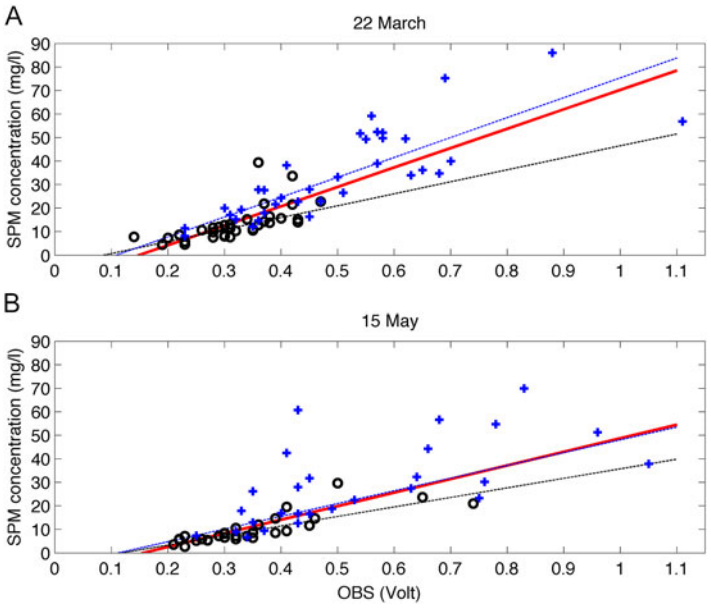

Fig. 2. OBS values against SPM concentrations. Black circles refer to surface samples; blue crosses to bottom samples. In each panel, the linear fit (red line) is based on surface and bottom data together. Also indicated are the fits for the subsets of surface (black dashed line) and bottom (blue dashed line) samples, taken separately.

https://doi.org/10.1017/njg.2014.7 Published online by Cambridge University Press

so that relatively more coarser-grained material was brought into suspension, to which OBS sensors respond less strongly. In other words, a higher concentration would be needed on 22 March than on 15 May to get the same OBS output. This explanation gains further plausibility if we look at fits for bottom or surface samples taken separately (in Fig. 2: blue and black dashed lines, respectively). For bottom samples the lines are steeper than for surface samples, implying that a higher concentration is needed for the former to get the same OBS value. This fits in with the fact that coarser-grained sediments (e.g. fine sand) are generally more prevalent near the bottom than near the surface. In addition, the OBS response is known to be sensitive to other properties, such as particle shape, near infrared reflectivity of the material ('color'), flocculation, phytoplankton blooms and more (Downing, 2006). One would need additional measurements to determine the importance of these factors in the specific setting.

Several sensitivity tests can be done, for example using separately the subsets of bottom and surface samples in constructing calibration lines, as indicated in Fig. 2. The gap between the lines then suggests a relative margin of uncertainty in the order of 15–20%.

Supplementing missing or noisy ADCP data

A downward looking 1.2 kHz RDI Workhorse ADCP was mounted at a pole on the R/V Navicula. It sampled over 88 bins of 0.5 m and a profile was logged every 3 s. Because of side-lobe interference, the ADCP data become noisy and unreliable in about the lowest 10% of the water column; for the deepest station 3, as much as the lowest 35% shows noisiness. These parts were replaced by the simple empirical profile proposed by van Veen (1937), $u = a\, h^{1/5.2}$, which he showed works well for the Vlie Inlet (here u is the velocity component, a is a constant chosen to fit the higher part of the profile and h is the height above the bottom).

The ADCP did not function during the first three casts on 22 March, so the profiles of stations 1 to 3 are missing from the first crossing. These were constructed heuristically by taking a linear combination of the profiles from the second and, close to a tidal period later, the last two crossings. As a test, we applied the same construction to stations 4 to 6: the resulting profiles bore a fair resemblance to the measured ones from these stations. In any case, concentrations of SPM were very low during this first crossing (as discussed below), so any error in these profiles is inconsequential for the overall SPM fluxes.

Reference levels for the vertical

Although the same stations 1 to 6 were visited during successive crossings, in practice this is only true in a loose sense, for the vessel cannot stay exactly at that position during the casts; moreover the CTD frame itself drifts away during its lowering and hoisting. This is one reason why the water depth recorded with the CTD frame is never the same during revisits of what is, nominally, the same station. The other reason, of course, is that from one visit to the next the surface height changes with the tide and variable wind surges. These two variable factors pose the problem of how to connect, for the same station, the vertical data points from different crossings.

We deal with these obstacles in the following way. It turns out that the ADCP was close to the true location of a station during at least some of the time of a cast. Thus, we select the N profiles that are closest to the station. Of these N profiles, we take the median for each vertical bin. We also take the median of the N values for the water depth measured by the ADCP (correcting for the fact that the ADCP hangs 1 m below the surface). From this median water depth we then subtract the elevation (with respect to NAP) as measured at Vlieland Haven, being the nearest tide-gauge station; we thus correct for the effect of tides and wind surges. After these corrections, only a slight variation remains in different casts for the same station. This must be due to the (small) variation in location between different casts, and the imprecision of the ADCP measurements themselves. Finally, we take, for each station, the median over all casts. We refer to this as the 'reference depth', the estimated water depth with respect to NAP.

This method appears to work well. Specifically, for 22 March, we choose $N = 10$. The distance of the selected profiles to their corresponding station is, on average, only 12 m, so the profiles can reasonably be considered to be taken 'at' the station. The reference depth is shown in Table 1, together with the standard deviation, which is a measure of the variation between different casts at the same station. Notice that in most cases this deviation is actually smaller than the bin size, so no better accuracy could be expected.

For 15 May, the ADCP data contained more noise, so we included more profiles: $N = 20$. The mean distance to corresponding stations was now 15 m. The reference shows a larger standard deviation, but, given these error bars, the median values are consistent with those of 22 March.

Finally, it is convenient to put all the measured variables of the vertical profiles into a fixed grid, to be used throughout. Integration over time then becomes particularly straightforward, since each specific gridpoint can be treated separately. Thus, we introduce a vertical axis on which, for each station, the bottom is fixed at a level $z = -h_b$, where h_b is the highest water level (i.e. the reference depth of that station plus high water). So, by definition, the water surface reaches $z = 0$ during high water, but lies lower at all other times. In the latter case, the gridpoints in between are assigned the value 'infinite' and are rendered white in the figures presented here (e.g. in Fig. 4). For time integrations concerning these gridpoints, there is no contribution from such moments.

We choose a vertical grid distance of 0.25 m (as in the CTD data), which is half that of the ADCP bin size. For each cast, the ADCP profile is filled into the new grid from the bottom

https://doi.org/10.1017/njg.2014.7 Published online by Cambridge University Press

upwards and interpolated to the finer grid size. At the top, data were missing in the upper 2 m, and this was filled up by constant extrapolation, i.e. assigning the upper value to the missing points above it, up to the level of the free surface during that cast. The CTD/OBS data are similarly filled in from below. Due to drifts of the ship and CTD frame, the frame may have landed at a deeper or shallower position than the station in question. In the former case, there are more data than needed for the grid and redundant data points are left out; in the latter case, there are not sufficient data and the missing near-surface values are filled in with constant extrapolation.

Thus, we work our way from the bottom upwards (instead of from the surface downwards), ensuring that the near-bottom values are included as correctly as possible, leaving extrapolations to near-surface values, which is the lesser evil so far as sediment transport is concerned.

Results

Spatial and temporal variations

We start by showing the results from the CTD/OBS casts in Fig. 3, which give a first impression of the spatial and temporal characteristics of the transports in the Vlie Inlet. We recall that the measurements of 15 May do not cover a full tidal cycle (missing the later flood stage) and have two transects less than

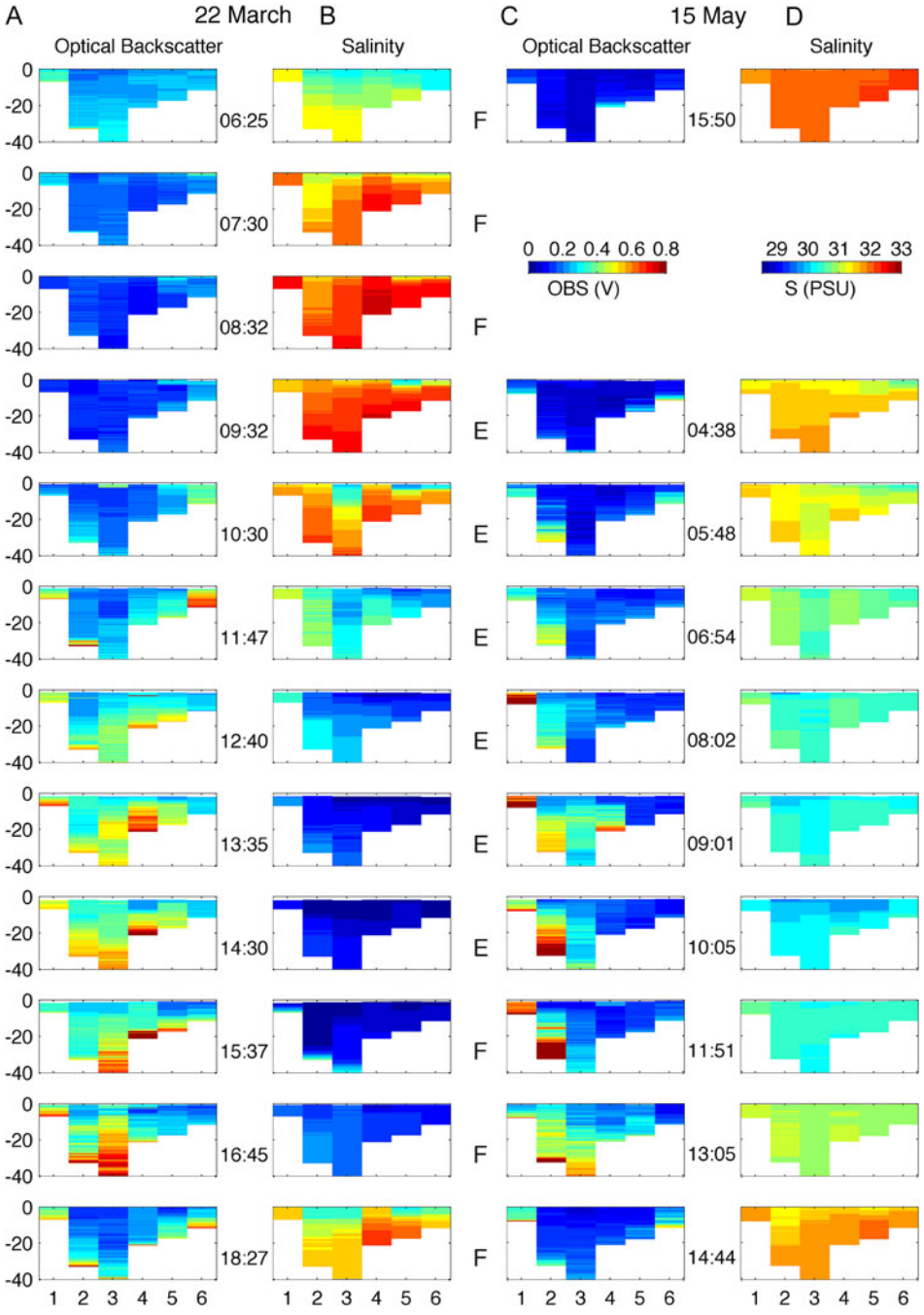

Fig. 3. Results from the CTD/OBS casts along the transect. For 22 March, time progresses from upper to lower panels, but for 15 May the panels have been slightly re-ordered to make the tidal phases correspond more closely to those of 22 March for easier comparison; thus, the last transect is plotted first. In each panel, the vertical indicates depth in metres; on the horizontal, the station number is given. The indicated time (in UTC) is the average during the crossing from stations 1 to 6. The phase of the tidal current is marked by E (ebb) and F (flood).Colour bars apply to both dates.

https://doi.org/10.1017/njg.2014.7 Published online by Cambridge University Press

on 22 March. We show OBS and salinity. The time of day is indicated in a cross-transect average sense; typically, the crossing from station 1 to 6 took about three quarters of an hour. The phase of the tide at that stage is indicated by E or F (ebb or flood).

Both for 22 March (panel columns a and b) and 15 May (panel columns c and d), a remarkable correspondence in the overall phases is seen between OBS and salinity: when the former is high, the latter is low, and vice versa.

The lowest values of salinity are seen during ebb, as expected since the fresh water from the landward side of the Vlie basin (mainly originating from the sluice at Kornwerderzand) is then exported. However, salinity stays low during the early stage of flood, which means that the relatively fresh water that was brought to the outer delta during ebb is being imported again at the beginning of flood. Conversely, relatively saline water is exported at the beginning of ebb.

During half of the tidal cycle – during late flood and early ebb – OBS values are low throughout. Only in the later stages of ebb do they rise, starting from the shallow sides of the channel. Then, the deepest part of the channel (stations 2 and 3) gains importance and finally becomes dominant at the beginning of flood, when high values are confined to those two stations. The broad picture is thus one of an export of SPM during late ebb, predominantly over the shallower sides adjacent to the intertidal flats, and a brief import through the central channel during early flood.

These measurements show how OBS varies locally (i.e. at this particular transect), but the origin of the signal, like that of fresh water, lies presumably farther into the basin. The main channels in the Wadden Sea are known to be predominantly sandy (van Straaten, 1964), so the (re)suspended sediments that pass the transect will generally have travelled some distance before they arrive at the transect. This idea gains plausibility from the fact that the OBS signal becomes strong only during the *second* half of the ebb phase. We can estimate the corresponding distance. With typical maximum current speeds of about 1.5 m s^{-1}, the tidal excursion is obtained by dividing this maximum by the (semidiurnal lunar) tidal frequency, giving about 10 km; this is the distance traversed by water parcels during the first half of ebb. The sediment that we see arriving at that point, therefore, must come from within a circle of about 10 km. The circle includes the intertidal flats adjacent to the Vliestroom and West Meep channels.

Meanwhile, clear differences are seen between the two campaigns. On 22 March, the distribution of OBS values is more or less symmetric across the channel, but on 15 May the pattern is strongly skewed towards its southwestern side (i.e. stations 1 and 2), suggesting that the supply comes now mainly from the western branch, Vliestroom, and adjacent intertidal flats. It is not evident whether this difference is due to wind direction or wind strength, although it is natural to expect that with the ENE winds on 22 March more sediment would be transported from the eastern flats and watershed into the West Meep, thus giving more supply to the eastern part of the main channel.

Local flux of SPM

The northern and eastern current velocities from the ADCP were rotated over an angle of 54.8° to transform the signal into cross- and along-transect components. The latter is typically five to ten times weaker than the cross-transect current; it would become still weaker if we reduced the angle slightly (by about 7°), indicating that our transect is not perfectly normal to the principal flow. This is, however, immaterial to the cross-transect transports that we calculate hereafter. For the cross-transect flow, we adopt the convention that negative values correspond to a flow into the Wadden Sea (flood) and positive values to a flow into the North Sea (ebb). Profiles coinciding with CTD casts were obtained as explained in the previous section. For each station the profiles were linearly interpolated (and where necessary extrapolated) to a 5-min timeline covering a full tidal period. (The duration of the tidal period is, in fact, intrinsically ambiguous; we examine this problem in the section *Discussion*.) This timeline is chosen to be the same for all stations, to facilitate comparisons between them. OBS values were treated similarly and translated into SPM concentrations via the calibration lines of Fig. 2.

The evolution of the cross-transect velocity and SPM concentration is shown in Fig. 4 for both campaigns. Each station has been given the same vertical extent in the panels, but notice that their water depths (and hence the vertical scales) vary greatly. This is also the reason why the white areas in the upper layer, marking the void due to low water, are more clearly visible in the outer panels, where the effect is relatively large because of the shallowness of the stations.

In Fig. 4, rows a and d, we see that the current amplitude decreases substantially from stations 1 to 6, while the phases hardly differ between the stations. In Fig. 4, rows b and e, SPM concentrations are plotted. The scale is limited at 60 g/m³; higher values are only sporadically reached. Here we see phase differences between the stations: the shallow stations generally precede the deeper ones with regard to peak values in SPM. In all cases the concentrations decrease strongly towards the surface. By contrast, the flux (Fig. 4c,f), obtained by multiplying current velocity and concentration, is on the whole rather more homogeneous in the vertical. This means that the upward decrease in concentration is largely offset by an upward increase in current velocity. (In cases when only surface data are available, it would thus make more sense to assume that the fluxes stay constant over the vertical than to assume this for SPM concentrations.) For the fluxes, the western half of the channel is dominant, especially so on 15 May. This skewness to the western side can be ascribed to two factors: first, tidal currents are stronger on the western side (Fig. 4a,d) and, second, phases of currents and SPM concentrations are more in unison

https://doi.org/10.1017/njg.2014.7 Published online by Cambridge University Press

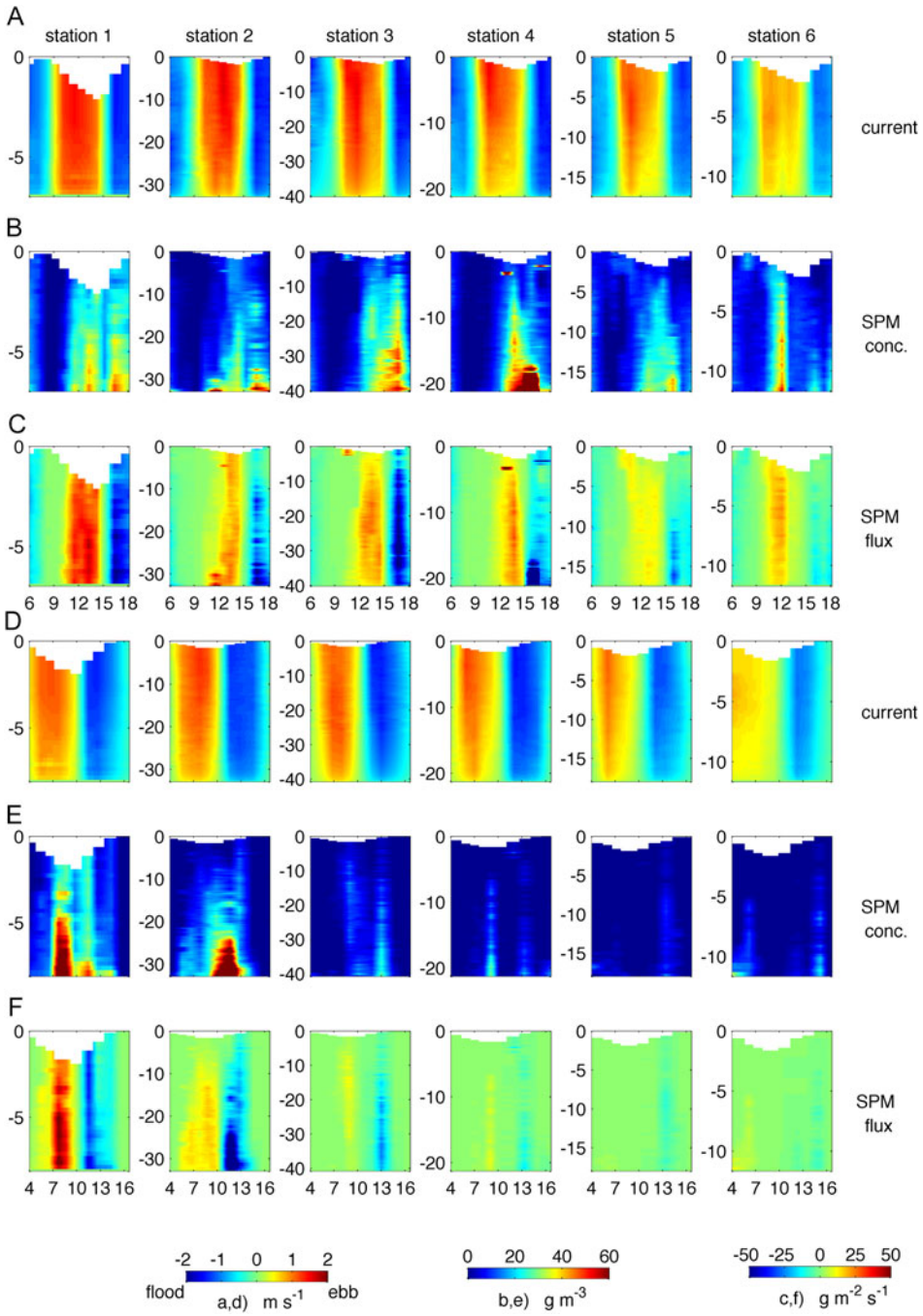

Fig. 4. Results for 22 March (rows a–c) and for 15 May (rows d–f): the cross-transect tidal current (rows a,d), the SPM concentration (rows b,e) and their product (rows c,f), based on linear interpolation of the data to 5-min intervals and extrapolation to a full tidal period. The six columns represent stations 1 to 6. In each panel, time is on the horizontal axis (hours UTC) and the depth with respect to HW (in metres) is on the vertical axis.

at western stations. For example, on 22 March (Fig. 4a,b), maximum concentrations occur around slack at station 4, whereas at station 1 maximum concentrations occur before and after slack, resulting in higher fluxes.

Tidal prism and transport of SPM

Starting from Fig. 4, rows c and f, we can now, for each station, vertically integrate the instantaneous fluxes and calculate the overall transport during ebb and flood. Thus, the real contribution from the different stations is cast into a more proper perspective. For example, station 1 has the highest local fluxes (see Fig. 4c,f), but due to its shallowness the contribution to the total transport is relatively modest (Fig. 5c,d). In all cases, stations 2 and 3 are predominant in the vertically integrated transports. Regarding the transport of water, a dominance of flood is found on both occasions (see black lines in Fig. 5a,b), but on 15 May it is more pronounced, which is not surprising in view of the strong NNW wind. In all panels there is a pronounced asymmetry, a skewness to the left (i.e. southwest), most clearly so for the SPM fluxes on 15 May (Fig. 5d).

Finally, we can horizontally integrate the results shown in Fig. 5; this yields the values gathered in Table 3. The water volumes differ between the two days of measurements.

https://doi.org/10.1017/njg.2014.7 Published online by Cambridge University Press

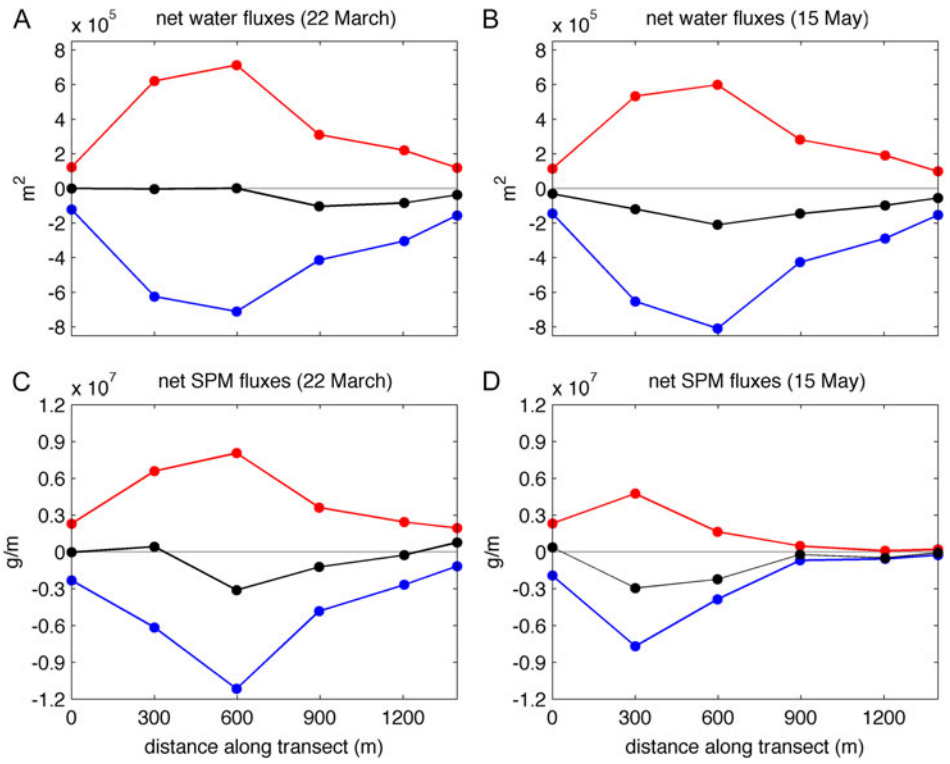

Fig. 5. Fluxes for water and SPM at stations 1 to 6 (from left to right), integrated over the vertical and in time for ebb and flood, separately. The timespans of ebb (red) and flood (blue) are integrated separately. The net result of the two is shown as the black line.

As expected, the NNW wind on 15 May reduced the export of water and increased the import.

Our values for the tidal prism are significantly smaller than earlier estimates for the *entire* inlet. These estimates, it should be noted, are themselves subject to a large margin of variability: reported values range from 880 million m³ (Postma, 1982) to 1078 million m³ (Louters & Gerritsen, 1994). Similar margins occur in an analysis by Hut (2004). These variations are to be expected: not only does the tide vary in intensity (e.g. spring-neap cycles), but the tidal prism (in spite of its name) is also strongly influenced by non-tidal effects, notably the wind, which causes it to be highly variable. In a numerical modelling study, covering two years with realistic forcing, Duran-Matute et al. (2014) found that the standard deviation of tidal prisms is typically about 20% of their long-term average (for the Vlie: 934 million m³). All reported values fall easily within that margin.

Our measurements cover only the main channel. Some idea of how much we miss (in comparison with the entire inlet) can be deduced from the different transects covered by Visser et al. (1986). They give values for a transect similar to ours, although it extended possibly somewhat farther to the east. That transect alone accounts for about 80% of the total tidal prism (Visser et al., 1986), so we may assume a similar percentage in our case. Extrapolated to the entire inlet, our average value for the tidal prism then approaches the lower bound of the range in the numerical study by Duran-Matute et al. (2014).

For the water volumes, a net import is seen on both days. This is qualitatively in agreement with data from the tidal gauge at Vlieland Haven, which showed a rise in sea level over each of the 13-hour periods (the rise can be largely ascribed to the diurnal inequality, along with wind effects on 15 May). There is a caveat, however, for the rise in level is not necessarily due to an inflow through the Vlie alone; other sources may have contributed, namely exchanges with the adjacent basins and discharges from the sluices. The latter is negligible for the dates we are concerned with here. It is in any case natural to assume that the Vlie Inlet must be the chief contributor; by lack of further data, we shall ignore the possible exchanges with the adjacent basins.

On 15 May, the tidal gauge at Vlieland Haven shows that the water level rose from +50 cm at the start of the campaign to +86 cm one tidal period later. For an estimated area of the Vlie basin of 668 km² (for mean high water, see Elias et al., 2012), this implies an overall import of -240×10^6 m³. This corresponds well with the net import we find for 15 May (-177×10^6 m³, following from Table 3), which, after extrapolation to the entire inlet, amounts to -221×10^6 m³. A margin

Table 3. The total exports during ebb and imports during flood of the water volumes and mass of SPM.

		Export	Import
22 March	Water (10^6 m³)	576	−633
	SPM (10^6 kg)	6.6	−7.8
15 May	Water (10^6 m³)	497	−674
	SPM (10^6 kg)	2.4	−4.1

https://doi.org/10.1017/njg.2014.7 Published online by Cambridge University Press

of error as small as 2% in the gross volumes would already be sufficient to accommodate the mismatch with the value derived from the tidal gauge.

A similar exercise can be done for 22 March; here the discrepancy is slightly larger: a net import of -71×10^6 m³ from Table 3 (after extrapolation to the entire inlet) compared to an imported volume of -107×10^6 m³ according to the rise in sea level at the tidal gauge. For the gross volumes, an uncertainty of 4% is now sufficient to resolve the discrepancy.

These comparisons show that the net tidal prisms are even quantitatively in good agreement with independent data from the tidal gauge. For the transport of SPM, however, the gross amounts are subject to a much larger range of uncertainty due to the conversion from OBS values to SPM concentrations (Fig. 2). Several sensitivity tests can be done, for example using only the bottom samples in constructing the calibration line. On that basis, we estimate that in the gross amounts, uncertainties may be as large as 20–30%. As a result, the net effect of import and export together must be regarded as unreliable, as it falls entirely within the margin of error. Qualitatively, however, a net import of sediment (as suggested by the values in Table 3) does make sense in our case; after all, along with the net import of water, one may expect an import of sediment.

Discussion: indeterminacy in the duration of the tidal cycle

In the preceding sections we have made reference to the *tidal cycle*. In practice, its duration is taken as the time between successive low waters, or between successive high waters, or between alternate slacks. However, these options produce different results. This problem seems to have received little attention in the literature; for this reason, we think it useful to include a short intermezzo on it here.

Naturally, the wind is a perturbing factor in this, but even if we restrict ourselves to purely tidal components, the ambiguity in the definition of 'the' tidal period persists. This unavoidable problem derives directly from the fact that the underlying astronomical periods (associated with the Earth's rotation on its axis, the yearly motion around the sun, the lunar period etc.) are incommensurable. For exactly the same reason it has been impossible to construct a calendar that truly reflects these astronomical periods.

By way of example, we use the tidal predictions for Vlieland Haven. By restricting ourselves to the predicted signal, we will be dealing only with tidal components and ignoring wind surges. In Fig. 6 we compare the time between successive low waters (red dots) with the time between successive high waters (blue dots) for the months of March to May 2012. Both are plotted as the shift with respect to the reference period of the semidiurnal lunar tidal period (M2, 12 h 25 min). The lunar phases of full and new moon are also indicated. Four things are apparent from this figure. First, the overall pattern follows the spring-neap cycle: times between successive low (or high) waters are generally shorter than the M2 period during spring tides (i.e. about two days after full or new moon), while they exceed the M2 period during neap tides, sometimes by as much as three quarters of an hour. (Thus, with regard to tidal prism, lower current amplitudes during neap tides are partially offset by the longer duration of its period.) Second, diurnal inequalities are clearly visible as up- and downward jumps in subsequent points of the same colour. Thus, not only the water level itself is affected by the diurnal inequality, but also the period. Third, even though the overall pattern is stamped by the spring-neap cycle, irregularities abound in the details– a manifestation of the aperiodic character of the tide, a direct result of the incommensurability of the underlying astronomical periods. Fourth – the most important point for the present discussion – the time between successive low waters is sometimes nearly identical to the time between successive high waters of that same day, but it can also be very different (by as much as half an hour). In the latter case, it becomes ambiguous how 'the' tidal period should be defined.

In the case at hand, we have for 22 March as the time between successive low waters 12 h 12 min, and between high waters 12 h 10 min. For 15 May the departure was larger: the time between successive low waters was 12 h 44 min and between high waters was 12 h 29 min. For both days we took the average for the duration of the time integration. With

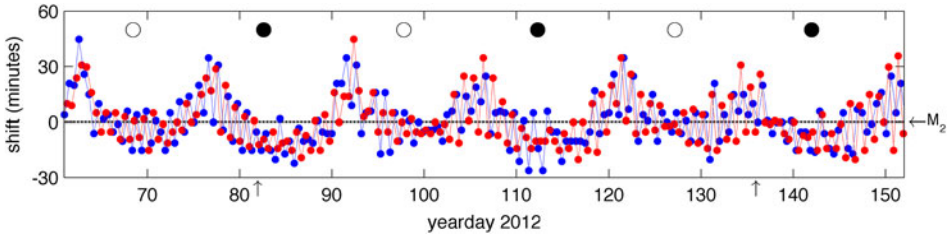

Fig. 6. The time between successive low waters (in red) and between successive high waters (in blue), shown as departures from the M_2 tidal period (horizontal grey line). These durations are based on tidal predictions for Vlieland Haven for the months of March to May. The campaigns described in this paper took place on yearday 82 (22 March) and 136 (15 May), as indicated by arrows. The lunar phases of full moon (open circle) and new moon (black circle) are also indicated.

https://doi.org/10.1017/njg.2014.7 Published online by Cambridge University Press

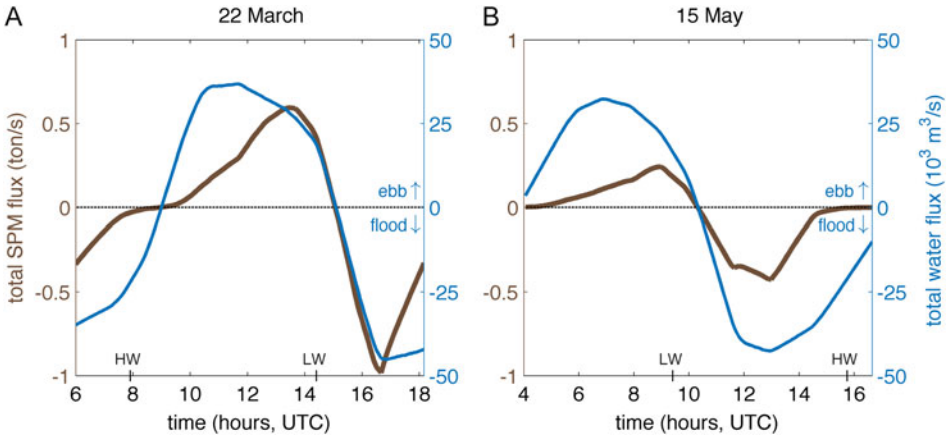

Fig. 7. Temporal evolution of the transports of SPM (brown) and water (blue), spatially integrated over the vertical plane of the transect.

regard to the transport of SPM, the problem can be somewhat mitigated by starting and ending the measurements at moments when concentrations are low; the integrated result is then less sensitive to the choice of the endpoint in time. As luck would have it, this is the case in our campaigns (cf. Fig. 3a,c).

Conclusion

In this study, the transport of water and SPM through the Vlie Inlet was examined using data from two measurement campaigns covering a tidal cycle, on 22 March and 15 May 2012. The conditions differed with respect to tides and wind, but common features can be identified. First, with regard to the spatial distribution, the transport of water and SPM is concentrated in the southwestern part of the deep channel (Fig. 5). This conforms to the asymmetric cross-channel bathymetry itself (Fig. 1). Second, a distinct pattern is found in the temporal evolution: SPM concentrations and transports are low during late flood and early ebb; the transport occurs predominantly before and after the slack from ebb to flood. This is further illustrated in Fig. 7, which condenses previous results by showing the spatially integrated transports of water and SPM as a function of time. The overall picture is that SPM starts to arrive at the inlet during the later stages of ebb, initially via the shallow sides adjacent to intertidal flats, is exported towards the outer delta, but returns at the beginning of flood via the deeper parts of the channel, after which the concentrations dwindle again. This suggests that the transports during the tidal cycle amount by and large to a reshuffling of SPM within the tidal basin, rather than to a genuine exchange between the North Sea and the Wadden Sea – an idea put forward already by Dronkers (1984).

In this respect there is a similarity with fresh water, which leaves during late ebb and (at least partially) returns during early flood (Fig. 2). Although no conclusions can be drawn from these measurements on the long-term net balance, an analysis using a realistic numerical model demonstrates that the Vlie plays indeed only a minor role in the net export of fresh water; instead, the key players are the Marsdiep and the watershed south of Terschelling (Duran-Matute et al., 2014). Future modelling studies may shed light on whether the Vlie plays a similarly minor role in the net transport of SPM. The Marsdiep, on the other hand, is known to have an import of SPM from the North Sea (Nauw et al., 2014). The Marsdiep is also the first tidal inlet encountered by the northward 'river' of silt along the Dutch coast (de Kok, 2004) and is thus (literally) in a more favourable position than the Vlie when it comes to sources of SPM.

Besides common features, notable differences between the campaigns also stand out in Fig. 7. The tidal currents were overall slightly stronger on 22 March than on 15 May (Fig. 7, blue lines), although for the flood phases this difference is masked by the effect of the strong NNW wind on 15 May. The difference in amounts of transport of SPM is much more pronounced (Fig. 7, brown lines): they are much smaller on 15 May. More insight into the origin of this difference is provided by the spatial view in Fig. 4: on 15 May less than half the channel (only the western side) contributes to the transport of SPM, as opposed to 22 March, when the entire channel is involved. A tentative explanation is that the eastern side may have received a supply of SPM from the eastern intertidal flats and adjacent watershed (via the channel West Meep, Fig. 1) due to ENE winds on 22 March, but not when the wind is NNW, as on 15 May. Numerical model simulations should be a useful tool to examine such possible dependences on wind direction in a systematic manner.

Acknowledgements

We thank the crew of the R/V *Navicula* for their assistance, Sven Ober for technical support and all who helped carrying out the measurements: Simona Aracri, Jurre de Vries, Meinard Tiessen and Matias Duran Matute. Carola van der Hout was supported by Ecoshape/BwN project NTW3.1. Janine Nauw was supported by ZKO project 83908230.

https://doi.org/10.1017/njg.2014.7 Published online by Cambridge University Press

References

Beets, D.J. & van der Spek, A.J.F., 2000. The Holocene evolution of the barrier and the back-barrier basins of Belgium and the Netherlands as a function of late Weichselian morphology, relative sea level rise and sediment supply. Netherlands Journal of Geosciences 79: 3-16.

de Kok, J.M., 2004. Slibtransport langs de Nederlandse kust. Bronnen, fluxen en concentraties. Report RIKZ/OS/2004.148w, Rijkswaterstaat (Den Haag): 25 pp.

Downing, J., 2006. Twenty-five years with OBS sensors: The good, the bad, and the ugly. Continental Shelf Research 26: 2299-2318.

Dronkers, J., 1984. Import of fine marine sediment in tidal basins. *In:* Laane, R.W.P.M. & Wolff, W.J. (eds): The role of organic matter in the Wadden Sea, Proceedings of the 4th International Wadden Sea Symp. Netherlands Institute for Sea Research, Publication Series 10-1984 (Texel): 83-105.

Duran-Matute, M., Gerkema, T., de Boer, G.J., Nauw, J.J. & Gräwe, U., 2014. Residual circulation and fresh-water transport in the Dutch Wadden Sea: a numerical modeling study. Ocean Science doi:10.5194/osd-11-197-2014, submitted.

Elias, E.P.L., van der Spek, A.J.F., Wang, Z.B. & de Ronde, J., 2012. Morphodynamic development and sediment budget of the Dutch Wadden Sea over the last century. Netherlands Journal of Geosciences 91: 293-310.

Hut, H.J., 2004. Stroommeting buitendelta zeegat tussen Vlieland en Terschelling 27 augustus 2002: project VLIEDEBI. Report DNN-AM-2003-212 (in Dutch). Rijkswaterstaat (Delfzijl): 19 pp.

Louters, T. & Gerritsen, F., 1994. Het mysterie van de wadden: hoe een getijdesysteem inspeelt op de zeespiegelstijging (in Dutch). Report RIKZ-94.040. Rijkswaterstaat (Den Haag): 70 pp.

Merckelbach, L.M. & Ridderinkhof, H., 2006: Estimating suspended sediment concentration using backscatterance from an acoustic Doppler profiling current meter at a site with strong tidal currents. Ocean Dynamics 56: 153-168.

Nauw, J.J., Merckelbach, L.M., Ridderinkhof, H. & van Aken, H.M., 2014. Long-term ferry-based observations of the suspended sediment fluxes through the Marsdiep inlet using acoustic Doppler current profilers. Journal of Sea Research 87: 17-29.

Postma, H., 1982. Hydrography of the Wadden Sea: movements and properties of water and particulate matter. Balkema (Rotterdam): 75 pp.

Sprent, P., 1993. Applied nonparametric statistical methods, 2nd edn. Chapman & Hall (London): 342 pp.

van Straaten, L.M.J.U., 1964. De bodem der Waddenzee (in Dutch). *In:* Abrahamse, J., Buwalda, J.D. & Van Straaten, L.M.J.U. (eds): Het Waddenboek. Thieme (Zutphen): 75-151.

van Straaten, L.M.J.U., 1975. De sedimenthuishouding in de Waddenzee (in Dutch). *In:* Swennen, C., De Wilde, P.A.W.J. & Haeck, J. (eds): Symposium Waddenonderzoek. Mededeling nr. 1 van de Werkgroep Waddengebied (Stichting-Veth, Arnhem): 5-20.

van Veen, J., 1937. Waarnemingen omtrent de snelheidsverdeeling in een verticaal. Rapporten en Mededeelingen van den Rijkswaterstaat, № 29 (in Dutch). Alg. Landsdrukkerij ('s Gravenhage): 45 pp.

Visser, C., de Graaff, N. & de Boer, M., 1986. Het vermogen van het Zeegat van het Vlie. Report ANW-86.H205 (in Dutch). Rijkswaterstaat (Hoorn): 20 pp.

Zagwijn, W.H., 1991. Nederland in het Holoceen, 2nd edn. Sdu (Den Haag): 46 pp.

https://doi.org/10.1017/njg.2014.7 Published online by Cambridge University Press